Turbulent bands in plane-Poiseuille flow at moderate Reynolds numbers

Xiangming Xiong, Jianjun Tao, Shiyi Chen, and Luca Brandt

Citation: Physics of Fluids (1994-present) **27**, 041702 (2015); doi: 10.1063/1.4917173
View online: http://dx.doi.org/10.1063/1.4917173
View Table of Contents: http://scitation.aip.org/content/aip/journal/pof2/27/4?ver=pdfcov
Published by the AIP Publishing

PHYSICS OF FLUIDS **27**, 041702 (2015)

Turbulent bands in plane-Poiseuille flow at moderate Reynolds numbers

Xiangming Xiong,[1] Jianjun Tao,[1,a)] Shiyi Chen,[1] and Luca Brandt[2]
[1]*SKLTCS and CAPT, IFSA Collaborative Innovation Center of MoE, Department of Mechanics and Engineering Science, College of Engineering, Peking University, Beijing 100871, China*
[2]*Linné Flow Centre and SeRC, KTH Mechanics, SE-100 44 Stockholm, Sweden*

(Received 26 December 2014; accepted 26 March 2015; published online 7 April 2015)

In this letter, we show via numerical simulations that the typical flow structures appearing in transitional channel flows at moderate Reynolds numbers are not spots but isolated turbulent bands, which have much longer lifetimes than the spots. Localized perturbations can evolve into isolated turbulent bands by continuously growing obliquely when the Reynolds number is larger than 660. However, interactions with other bands and local perturbations cause band breaking and decay. The competition between the band extension and breaking does not lead to a sustained turbulence until Re becomes larger than about 1000. Above this critical value, the bands split, providing an effective mechanism for turbulence spreading. © *2015 AIP Publishing LLC*. [http://dx.doi.org/10.1063/1.4917173]

Subcritical transition triggered by finite-amplitude perturbations in viscous shear flows has been a long-standing open problem since the experimental work of Reynolds in 1883.[1] The pressure-driven Hagen-Poiseuille flow (HPF), plane-Poiseuille flow (PPF), and the shear-driven plane-Couette flow (PCF) are three typical canonical shear flows commonly examined. In contrast to channel flows extending infinitely in the spanwise direction, the transition in pipe flow may be analysed with a one-dimensional model,[2] and several stages of the transition process have been identified numerically and experimentally.[3–5] As concerning channel flows, the shear-driven plane-Couette flow has a linear velocity profile, i.e., the base-flow velocity gradient is uniform along the transverse direction and has been extensively investigated as well (for reviews, we refer to Refs. 6–8). It is found that localized turbulence, e.g., puffs in HPF and turbulent bands or stripes in PCF, plays an important role during the transition to sustained turbulence.

Early experiments in plane Poiseuille flow revealed that turbulent bursts first occur at a Reynolds number of about 1000.[9–12] The Reynolds number is defined as $Re = U_c h/\nu$, where U_c is the centerline velocity of the base flow, h is the half channel height, and ν is the kinematic viscosity of the fluid. Later studies focused on higher Reynolds number flows ($Re \geq 1000$): turbulent spots and their characteristics have been thoroughly studied[13–17] and, more recently, numerical simulations revealed the presence of closely arranged turbulent bands or stripes.[18,19] The flow structures at moderate Reynolds numbers have been revisited lately.[20] In order to simplify the spatio-temporal complexity of PPF and reduce the computational costs, slender computational domains at fixed tilt angles to the streamwise direction have been used to simulate band patterns at moderate Reynolds numbers.[21,22] It should be noted that in the previous studies of PPF, the turbulent band always interacted with its neighbours (e.g., other bands and local patches) or with itself due to the periodic boundary conditions imposed in the narrow computational domains. Consequently, the long-term behaviour of an isolated turbulent band (ITB) is still unknown, and this is the main motivation of this letter.

The incompressible Navier-Stokes equations are solved with a spectral code,[23] where the velocity field is expanded in Fourier modes in the streamwise x-direction and spanwise z-direction and

a)Author to whom correspondence should be addressed. Electronic mail: jjtao@pku.edu.cn.

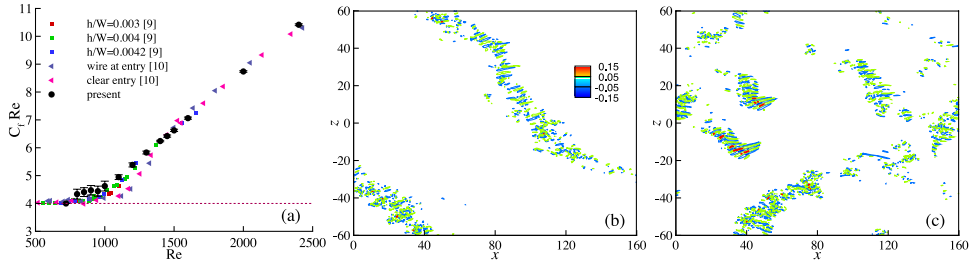

FIG. 1. (a) ReC_f as a function of Re from the present simulations and previous experiments. Error bars indicate the range of temporal variation in 4000 time units; the horizontal dashed line represents the laminar state value. h/W is the aspect ratio of the cross section of the experimental channel. (b) and (c): iso-contours of the transverse velocity at the midplane after 10 000 time units for Re = 950 and 1000, respectively.

Chebyshev polynomials in the wall-normal or transverse direction y. The boundary conditions in the x and z directions are therefore periodic, with no-slip conditions imposed at the walls ($y = \pm h$). U_c and h are chosen as the characteristic velocity and the length scale, respectively. The dimensionless flow rate is kept constant during the simulations. We use $(n_x, n_y, n_z) = (768, 65, 1024)$ spectral modes in a domain of size $(L_x, L_y, L_z) = (160h, 2h, 120h)$. The accuracy of the present results is verified by comparing with simulations in a domain of size $(320h, 2h, 240h)$ with the same spectral accuracy at Re = 1000. The difference of the friction factor $C_f = 2\tau_w/\rho U_c^2$ was found to be less than 0.5%, where τ_w is the averaged wall shear stress. It is shown in Fig. 1(a) that the simulation results at Reynolds numbers in the range $1300 \le \mathrm{Re} \le 2400$ agree well with available experimental data.[9,10]

The data reported in Fig. 1 are obtained starting with a statistically steady turbulent state at Re = 2000 and then decreasing the Reynolds number gradually. Three main observations from the data in Fig. 1 are worth further discussion. First, C_f does not increase greatly until Re > 1000, and, indeed, the flow patterns are different for Re below and above 1000. Long and isolated band-type structures can be observed at Re = 950 even after 10 000 time units (Fig. 1(b)), while the flow is spatially intermittent as shown in Fig. 1(c) at Re = 1000. Second, the skin friction C_f varies stochastically as shown by the error bars in the figure for 700 < Re < 1000. Third, the disturbed flow returns to the laminar state for Reynolds numbers below 700. In order to understand the underlying physical mechanisms, we complete the analysis performed from initially turbulent fields with the study of how a localized disturbance evolves to sustained turbulence.

The temporal evolution of a localized disturbance at Re = 900 is illustrated in Fig. 2; the simulation is performed in a computational domain of size $(L_x, L_y, L_z) = (100h, 2h, 80h)$ using (512,

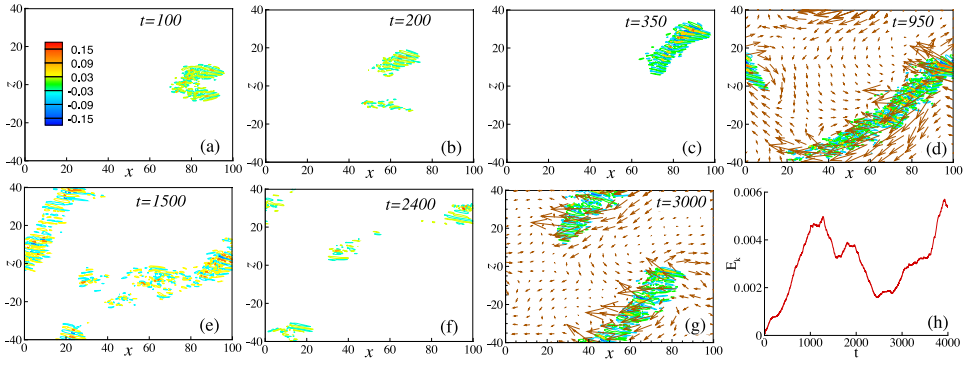

FIG. 2. The formation, transient growth, and break-up of an isolated turbulent band triggered by a localized disturbance at Re = 900. The iso-contours of the transverse velocity are shown in the midplane. The in-plane disturbance velocity is depicted by vectors on a coarse mesh in (d) and (g) to illustrate the large-scale flow around the band. The time series of the volume-averaged disturbance kinetic energy E_k is shown in (h).

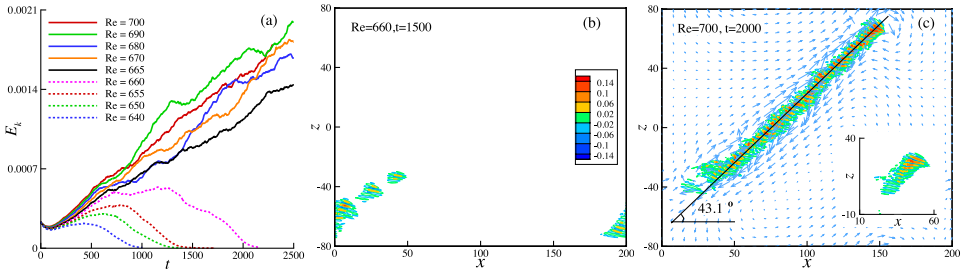

FIG. 3. (a) Time series of the volume-averaged disturbance kinetic energy E_k at different Reynolds numbers and for the same initial condition. The iso-contours of the transverse velocity in the midplane are shown in (b) and (c), where the initial perturbation pattern is added as an inset. The mean velocity of disturbance in the plane at y = 0.514 is depicted by vectors on a coarse mesh to show the large-scale flow.

65, 512) spectral modes. At time t = 100, we find a turbulent patch with separate upper and lower parts (see Fig. 2(a)). These two parts move in opposite spanwise direction, and depending on the specific details of the disturbance one or both of them may quickly decay. For the case shown in Fig. 2(a), the upper part survives (see Fig. 2(b)) and evolves into a short oblique band at t > 250 as shown in Fig. 2(c). This band is composed of smaller-scale perturbations illustrated by iso-contours of the transverse velocity and surrounded by a large-scale laminar flow region depicted by the instantaneous velocity vectors in Fig. 2(d). The large-scale flow is illustrated more clearly later (cf. Fig. 3(c)) by examining the mean disturbance fields.

The mechanism for the growth in the oblique direction is similar to that of PCF,[24–26] where the large-scale motions play the key role. At t = 950, a long band is formed (see Fig. 2(d)) and the volume-averaged disturbance kinetic energy E_k is close to its maximum value as shown in Fig. 2(h). Unlike the PPF, the basic state of PCF has velocities in opposite directions on each channel half, and hence, the perturbations extend in a zigzag style.[25] When the band is long enough, its two ends are close to each other due to the periodic boundary conditions, and the interactions between the large-scale flows around the ITBs cause band breaking as reported in Fig. 2(e). Some broken pieces decay (Fig. 2(f)) and E_k decreases (see Fig. 2(h)). On the other hand, some residues of the broken band may trigger new stripes (Fig. 2(g)), which leads to a new increase of E_k (see energy evolution in Fig. 2(h)). Therefore, the oscillations of E_k shown by the error bars in Fig. 1 and in Fig. 2(h) are caused by the competition between the band breaking and band extension.

According to our simulations, the band with a positive oblique angle relative to the streamwise direction is surrounded by a clockwise large-scale flow (Fig. 2(d)), and those with a negative angle are associated to an anti-clockwise circulation. Consequently, these large-scale motions tend to push parallel coherent structures to tilt away, and hence, they are here referred to as ITB.

A natural question about ITB then arises: is this a transient phenomenon?

In order to answer this question, we enlarge the computation domain to the size $(L_x, L_y, L_z) = (200h, 2h, 160h)$ (with a resolution of (1024, 65, 1024) spectral modes), so that the ITB can evolve longer without being affected by the periodic boundary conditions. In addition, in order to study its own dynamic behaviour, ITB should not be affected by other bands or perturbations. Therefore, the snapshot at t = 300 of the Re = 900 case (similar to the flow in Fig. 2(c)) was used as the initial flow field and the simulation results are shown in Fig. 3. This initially localized structure is not a typical spot but an isolated turbulent band, which is still very short and can be used as a "seed" of ITB. When Re ≤ 660, ITB extends obliquely first, leading to an increase of the volume-averaged kinetic energy of the disturbance E_k (Fig. 3(a)), but the elongated structure cannot be sustained and instead breaks into smaller patches as shown in Fig. 3(b), indicating a complete transient phenomenon, as also found in other spatially extended systems.[27] For Re > 660, E_k increases continuously (see Fig. 3(a)) and the ITB "seed" can extend to a very long turbulent band as shown by the visualization in Fig. 3(c). According to the data obtained at t = 2000 and Re = 700 (Fig. 3(c)), the Re_τ defined with the friction velocity is 38, and the corresponding mesh spacings Δx^+, Δy^+, and Δz^+ are 7.43, 0.046–1.87, and 5.94, respectively. The resolution used here is finer than that used for fully developed turbulent channel flows.[28] Since spots either decay or develop to turbulent bands, they have

much shorter lifetime than ITB. Therefore, the ITB and not the spot is the typical coherent structure of transitional PPF at moderate Reynolds numbers for large enough domains.

Three additional features shown in Fig. 3 are worth further discussing. First, the mean field shows clearly a large-scale clockwise flow surrounding the turbulent band. Since the ITB both extends obliquely and moves downstream with time, the mean flow is calculated by averaging over 100 snapshots with a time step of 0.7, where the data are shifted back in the upstream direction with the ITB advection velocity $U_a = 0.736$. Note that the mean flow vectors are shown not in the midplane but in the wall-parallel plane at $y = 0.514$, where the base flow velocity is equal to U_a. It is found that U_a is a weak function of Re. Second, the tilt angle changes with the Reynolds number. Similar as shown in Fig. 3(c), the tilt angles of the ITBs at Re = 680, 690, 700, 800, and 850 are estimated to be 38.6°, 40.1°, 43.1°, 43.4°, and 42.9°, respectively. Third, an isolated turbulent band can extend continuously and obliquely $140h$ in 2000 time units at Re = 700 while keeping its streamwise and spanwise lengths and the tilt angle statistically constant. Note that in a smaller computational domain, an ITB has broken into segments by t = 1500 as shown in Fig. 2(e) due to the band interaction caused by the periodic boundary conditions. Based on the above observations, it is expected that the oblique extension will continue for Re > 660 if the computational domain is large enough and there are no other perturbations in the neighbourhood of the ITB to induce breaking or quenching.

Besides the Reynolds number, the initial disturbance amplitude or kinetic energy has an important impact on the ITB's lifetime. Since the mean disturbance kinetic energy in the cross section is almost the same along an ITB, longer ITB corresponds to larger E_k as shown in Fig. 3. The solutions at Re = 665 obtained in Fig. 3 are used as initial flow fields to study the pattern evolution at lower Reynolds numbers, namely, Re = 660, 650, and 640. It is shown in Fig. 4 that a larger initial E_k is required to maintain a continuous increase of E_k or the band extension at a lower Reynolds number. In other words, there is a critical perturbation kinetic energy (as shown by the grey horizontal bar in Fig. 4) for a band to survive at each Reynolds number, which increases when decreasing Re and below which the ITB is a transient phenomenon. According to Fig. 3(a), the maximum E_k during the transient growth process increases with Re, but the "seed" ITB still cannot reach the critical E_k level and decay eventually until Re ≥ 665. This result explains the experimental phenomenon reported in Fig. 1 that C_f slightly deviates from the laminar value only as Re > 667.5.[9]

As discussed in Fig. 2(a), statistically steady state cannot be obtained at Re = 900 due to the band interactions. Similarly, a simulation of plane-Couette flow showed that the turbulent fraction did not converge to a statistically steady value at Re = 325.[25] In this letter, we used more samples to study the long-term effect of band interaction on the volume-averaged kinetic energy of the whole flow field. A flow state similar to that depicted in Fig. 2(e) was first obtained at $Re = 1000$, then 20 transient states were used as the initial fields to investigate the survival probability P of the localized turbulence at 700 ≤ Re ≤ 950, and the results are shown in Fig. 5. Because of the cost of such long simulations in large domains, the sample size is somewhat limited; however, the probability P does increase with Re. The localized turbulence can remain at Re = 700 but the lifetime is less than 2500 time units for all our simulations. Conversely, the perturbations may survive quite long (e.g., more

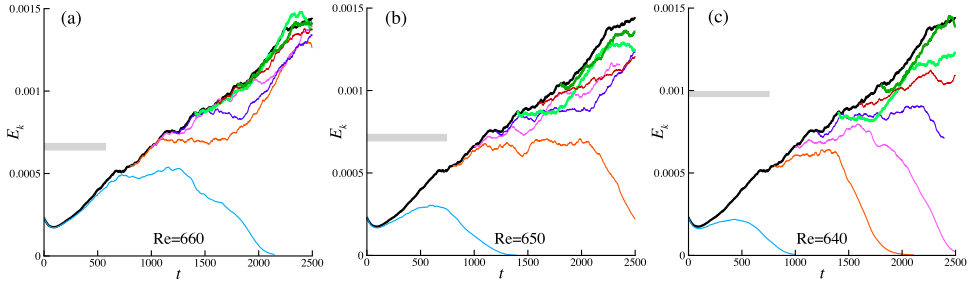

FIG. 4. (a)-(c) Time series of E_k at different Reynolds numbers. Different colours indicate the simulations with different initial flow fields, which are the solutions of Re = 665 (black line) at t = 0, 800, 1000, 1200, 1400, 1600, and 1800. The horizontal grey bars denote the critical E_k for the ITB to survive.

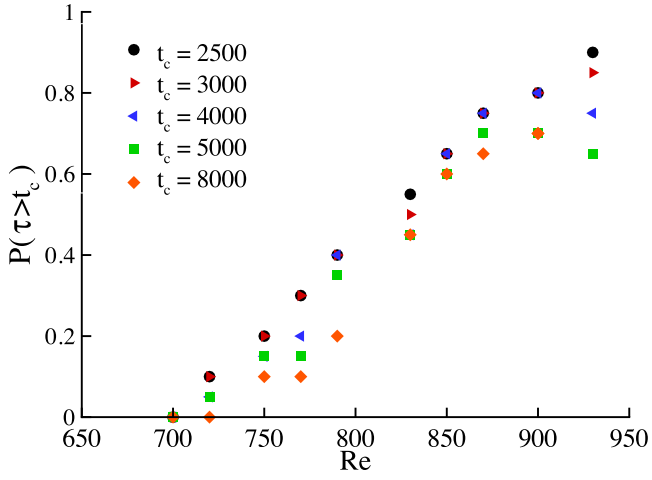

FIG. 5. Survival probability P (lifetime $\tau > t_c$) of the turbulent bands at moderate Re. τ is the computation time before the volume-averaged kinetic energy of disturbance is less than 10^{-4}.

than 8000 time units) if Re > 720 but they are yet not self-sustained when Re is as high as 950, where $P(\tau > 8000)$ is still less than 1.

Based on the above analyses, now, we can explain why it is still difficult to observe a significant increase of the mean flow properties (e.g., E_k or C_f) in experiments[9,10] if Re is just above 660. The reason is twofold. First, randomly distributed boundary disturbances (e.g., boundary roughness) and strong upstream perturbations may lead to multiple spots and bands. The interactions among them may cause band breaking and subsequent decay of these localized disturbances. Second, the initial disturbances used in the experiments are not the well-developed turbulent bands used in our simulations (Figs. 3 and 4), and the time required by different initial disturbances to evolve into spots and bands is different. In addition, the streamwise distance between measurement points was not long enough for the turbulent structures to be fully developed at moderate Reynolds numbers.[9,10] Consequently, the mean properties of these developing flows only slightly deviate from their laminar values and are still strongly dependent on the entry or upstream (disturbance) conditions and the aspect ratios of the flow channels as shown in Fig. 1.

The solution obtained at t = 1000 for the case of Re = 700 discussed in Fig. 3 is used as initial field to study how an ITB leads to sustained turbulence. It is shown in Fig. 6 that at t = 200, the ITB remains an isolated one at Re = 950 but splits at Re = 1100, as indicated by the red circles in the figure. In fact, band split occurs later also in the case of Re = 950 (e.g., at t = 800), but the new-born bands decay soon, and hence, only one isolated band is found at t = 2000. The flow

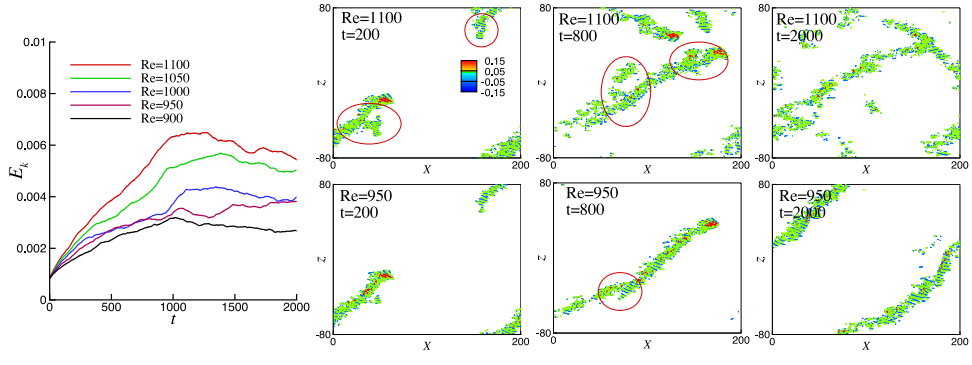

FIG. 6. Temporal evolutions of the same ITB at different Reynolds numbers. E_k as a function of time is shown on the left, and the iso-contours of the transverse velocity in the midplane at different Re and time are shown on the right. The red circles indicate the regions of band split.

pattern (Re = 950 and t = 2000) is similar to that shown in Fig. 1(b) except that the ITBs tilt at opposite angles due to different initial perturbations. In contrast to the case at Re = 950, the band split happens more frequently for Re = 1100 and produces more band "seeds". Consequently, the flow field becomes spatially intermittent at t = 2000 as shown in Fig. 6 similar pattern as in Fig. 1(c). According to the present simulations, the turbulence spreading caused by oblique extension and band split is found to overcome the decay process when Re > 1000. As a result, the turbulence is temporally sustained and the mean properties (e.g., C_f) deviate clearly from the corresponding laminar values. This critical value of the Reynolds number is consistent with experimental observations. For example, Nishioka and Asai[12] found that turbulence could not be self-sustained for Re below 1000. Similarly, it has been found in Hagen-Poiseuille flow that a competition between puff split and puff decay determines a threshold for sustained turbulence.[29]

It has been revealed in PCF and HPF that a small domain size has a noticeable effect on the lifetime of turbulence.[7,30] For PPF, we tested different widths at Re = 900 and found that the turbulent bands could not be formed when the domain width was reduced to $40h$. A recent experimental study showed that perturbations induced by continuous jets did not trigger subcritical transition in PPF below Re = 1500,[31] where the width of the test section was $15h$. Recently, slender and tilted computational domains were used to study the flow patterns at different transition stages in PPF[21,22] and the splitting phenomenon of PCF.[32] It should be noted that such slender domains cannot describe some important behaviours of ITB, e.g., band extension and band breaking. In addition, in a slender domain, all turbulent bands or stripes tilt in the same direction, while it is found that the band produced by splitting may have an opposite tilt angle in a large computational domain, as shown in Fig. 6 (Re = 1100 and t = 200).

In this letter, the subcritical transition scenario of plane-Poiseuille flow is numerically simulated in large computational domains. The isolated turbulent band, instead of the spot, is found to be the key coherent structure dominating the initial stage of the transition. At low Reynolds numbers, the ITB extends obliquely and then decays by band breaking. When Re > 660, short ITB can grow until interacting with other perturbations. Sustained turbulence is observed above Re = 1000, where the band splitting enhances significantly the spreading of turbulence.

We would like to thank F. H. Busse and many cited authors for insightful discussions. The simulations were performed on TianHe-1(A), and this work has been supported by the National Natural Science Foundation of China (Nos. 11225209 and 10921202).

[1] O. Reynolds, "An experimental investigation of the circumstances which determine whether the motion of water shall be direct or sinuous, and of the law of resistance in parallel channels," Proc. R. Soc. London **35**, 84 (1883).
[2] D. Barkley, "Simplifying the complexity of pipe flow," Phys. Rev. E **84**, 016309 (2011).
[3] B. Eckhardt, T. M. Schneider, B. Hof, and J. Westerweel, "Turbulence transition in pipe flow," Annu. Rev. Fluid Mech. **39**, 447-468 (2007).
[4] B. Eckhardt, "A critical point for turbulence," Science **333**, 165-166 (2011).
[5] T. Mullin, "Experimental studies of transition to turbulence in a pipe," Annu. Rev. Fluid Mech. **43**, 1-24 (2011).
[6] P. Manneville, "Understanding the sub-critical transition to turbulence in wall flows," Pramana **70**, 1009-1021 (2008).
[7] L. S. Tuckerman and D. Barkley, "Patterns and dynamics in transitional plane Couette flow," Phys. Fluids **23**, 041301 (2011).
[8] P. Manneville, "On the growth of laminar–turbulent patterns in plane Couette flow," Fluid Dyn. Res. **44**, 031412 (2012).
[9] S. J. Davies and C. M. White, "An experimental study of the flow of water in pipes of rectangular section," Proc. R. Soc. A **119**, 92-107 (1928).
[10] V. C. Patel and M. R. Head, "Some observations on skin friction and velocity profiles in fully developed pipe and channel flows," J. Fluid Mech. **38**, 181-201 (1969).
[11] D. R. Carlson, S. E. Widnall, and M. F. Peeters, "A flow-visualization study of transition in plane Poiseuille flow," J. Fluid Mech. **121**, 487 (1982).
[12] M. Nishioka and M. Asai, "Some observations of the subcritical transition I plane Poiseuille flow," J. Fluid Mech. **150**, 441-450 (1985).
[13] F. Alavyoon, D. S. Henningson, and P. H. Alfredsson, "Turbulent spots in plane Poiseuille flow-flow visualization," Phys. Fluids **29**, 1328-1331 (1986).
[14] F. Li and S. E. Widnall, "Wave patterns in plane Poiseuille flow created by concentrated disturbances," J. Fluid Mech. **208**, 639-656 (1989).
[15] D. Henningson, P. Spalart, and J. Kim, "Numerical simulations of turbulent spots in plane Poiseuille and boundary layer Flow," Phys. Fluids **30**, 2914-2917 (1987).
[16] D. S. Henningson and J. Kim, "On turbulent spots in plane Poiseuille flow," J. Fluid Mech. **228**, 183-205 (1991).
[17] D. S. Henningson, A. V. Johansson, and P. H. Alfredsson, "Turbulent spots in channel flows," J. Eng. Math. **28**, 21-42 (1994).

[18] T. Tsukahara, Y. Seki, H. Kawamura, and D. Tochio, "DNS of turbulent channel flow at very low Reynolds numbers," in *Proceedings of the 4th International Symposium on Turbulence and Shear Flow Phenomena*, *Williamsburg, VA, USA*, *June 2005*, pp. 935-940; e-print arXiv:1406.0248 [physics.flu-dyn].
[19] T. Tsukahara, Y. Kawaguchi, H. Kawamura, N. Tillmark, and P. H. Alfredsson, "Turbulence stripe in transitional channel flow with/without system rotation," in *Proceedings of the IUTAM Symposium on Laminar-Turbulent Transition* (Stockholm, Sweden, 2009).
[20] J. Tao and X. M. Xiong, "The unified transition stages in linearly stable shear flows," in *Proceedings of the 14th Asian Congress of Fluid Mechanics*, *Hanoi and Halong, Vietnam*, *October 2013* (Science and Technology, 2013), pp. 55-62.
[21] L. S. Tuckerman, "Turbulent-laminar banded patterns in plane Poiseuille flow," Proceedings of the 23rd International Congress of Theoretical and Applied Mechanics, Beijing, China, 19–24 August 2012.
[22] L. S. Tuckerman, T. Kreilos, H. Schrobsdorff, T. M. Schneider, and J. F. Gibson, "Turbulent-laminar patterns in plane Poiseuille flow," Phys. Fluids **26**, 114103 (2014).
[23] M. Chevalier, P. Schlatter, A. Lundbladh, and D. S. Henningson, "SIMSON a pseudo-spectral solver for incompressible boundary layer flows," Technical Report TRITA-MEK 2007:07, 2007.
[24] J. J. Hegseth, "Turbulent spots in plane Couette flow," Phys. Rev. E **54**, 4915-4923 (1996).
[25] Y. Duguet, P. Schlatter, and D. S. henningson, "Formation of turbulent patterns near the onset of transition in plane Couette flow," J. Fluid Mech. **650**, 119 (2010).
[26] Y. Duguet and P. Schlatter, "Oblique laminar-turbulent interfaces in plane shear flows," Phys. Rev. Lett. **110**, 034502 (2013).
[27] T. Tél and Y. C. Lai, "Chaotic transients in spatially extended systems," Phys. Rep. **460**, 245-275 (2008).
[28] J. Kim, P. Moin, and R. Moser, "Turbulence statistics in fully developed channel flow at low Reynolds number," J. Fluid Mech. **177**, 133-166 (1987).
[29] K. Avila, D. Moxey, A. de Lozar, M. Avila, D. Barkley, and B. Hof, "The onset of turbulence in pipe flow," Science **333**, 192 (2011).
[30] T. M. Schneider and B. Eckhardt, "Lifetime statistics in transitional pipe flow," Phys. Rev. E **78**, 046310 (2008).
[31] G. Lemoult, J.-L. Aider, and J. E. Wesfreid, "Experimental scaling law for the subcritical transition to turbulence in plane Poiseuille flow," Phys. Rev. E **85**, 025303 (2012).
[32] L. Shi, M. Avila, and B. Hof, "Scale invariance at the onset of turbulence in Couette flow," Phys. Rev. Lett. **110**, 204502 (2013).